BASIC RESEARCH

Evaluation the Scanning Accuracy of Blue-Light Laboratory Scanners in Complete Edentulous Maxilla with Multiple Implants with Titanium Scan Bodies

Evaluación de la precisión de escaneado de los escáneres de laboratorio de luz azul en maxilares desdentados completos con implantes múltiples con cuerpos de escaneado de titanio

Bahadır Ezmek DDS, MSc, PhD¹; Osman Cumhur Sipahi DDS, PhD²

1. Department of Prosthodontics, Gulhane Faculty of Dentistry, Health Sciences University, Ankara, Turkey. https://orcid.org/0000-0002-1651-3260
2. Department of Prosthodontics, Gulhane Faculty of Dentistry, Health Sciences University, Ankara, Turkey. https://orcid.org/0000-0002-6808-2976

Correspondence to: Dr. Bahadir Ezmek - bezmek@gmail.com

ABSTRACT: To evaluate the accuracy of complete arch scanning with multiple implant titanium scan bodies using laboratory scanners. A master model of an edentulous maxillary arch with 6 implants was fabricated. Titanium scan bodies were inserted into the model. Three laboratory scanners were used: D2000 (3Shape), Vinyl High Resolution (Smart Optics), and inEos X5 (Dentsply Sirona). The master model was consecutively scanned ten times using dental laboratory scanners (LS) without detaching and repositioning the scan bodies. Linear and angular accuracy between adjacent implants was measured using inspection software (Control X, Geomagic). The accuracy of the complete arch scans was calculated. Implant regions were defined as; parallel (R1: #24-26 and #16-14), angled (R2: #22-24 and #14-12), angled to occlusal plane (R3: #12-22), and cross-arch (R4: #16-26). The effect of LS and implant region on accuracy was compared using two-Way ANOVA (α=0.05). Significant greater linear distortion was noted in R4 (61.2±17.9µm) compared to R1 (23.4±15.5µm) and R2 (26±17.7µm) (p<0.01). Greater linear distortions were noted in R4 with D2000 (0.07±0.016 degrees) and Vinyl High Resolution (0.067±0.02 degrees) than inEos X5 (0.032±0.021 degrees) (p>0.05). Greater mean linear precisions were noted in R1 (9±8µm) and R3 (9.3±8.3µm) than R4 (12.6±10.3µm) (p<0.05). The highest linear precision was noted in D2000 (7.2±7.6µm) (p<0.05). The angular precision of D2000 (0.02±0.015 degrees) was the highest (p<0.01). The angular precision

EZMEK B., SIPAHI O.C., 2023: Evaluation the Scanning Accuracy of Blue-Light Laboratory Scanners in Complete Edentulous Maxilla with Multiple Implants with Titanium Scan Bodies.-ODOVTOS-Int. J. Dental Sc., 25-3 (September-December): 55-66.

ODOVTOS-Int. J. Dent. Sc. | No. 25-3: 55-66, 2023 | ISSN: 2215-3411. 55

of R4 (0.036±0.018 degrees) was the lowest (p<0.01). This study revealed that the trueness was affected by the implant region and the precision was affected by both LS and implant region.

KEYWORDS: Digitalization; Scan accuracy; Laboratory scanners; Titanium scan body; Multi-unit abutment; Complete arch.

RESUMEN: Evaluar la precisión del escaneado de la arcada completa con cuerpos de escaneado de titanio de múltiples implantes utilizando escáneres de laboratorio. Se fabricó un modelo maestro de una arcada maxilar edéntula con 6 implantes. Se insertaron cuerpos de escaneo de titanio en el modelo. Se utilizaron tres escáneres de laboratorio: D2000 (3Shape), Vinyl High Resolution (Smart Optics) e inEos X5 (Dentsply Sirona). El modelo maestro se escaneó consecutivamente diez veces usando escáneres de laboratorio dental (LS) sin separar y reposicionar los cuerpos de escaneo. La precisión lineal y angular entre implantes adyacentes se midió utilizando un software de inspección (Control X, Geomagic). Se calculó la precisión de los escaneos completos del arco. Las regiones del implante se definieron como; paralelo (R1: #24-26 y #16-14), angulado (R2: #22-24 y #14-12), angulado al plano oclusal (R3: #12-22) y cruzado (R4: #16-26). El efecto de LS y la región del implante en la precisión se comparó mediante ANOVA de dos vías (α=0,05). Se observó una distorsión lineal significativamente mayor en R4 (61,2±17,9µm) en comparación con R1 (23,4±15,5µm) y R2 (26 ±17,7µm) (p<0,01). Se observaron mayores distorsiones lineales en R4 con D2000 (0,07±0,016 grados) y vinilo de alta resolución (0,067±0,02 grados) que en inEos X5 (0,032±0,021 grados) (p>0,05). Se observaron precisiones lineales medias mayores en R1 (9±8µm) y R3 (9,3±8,3µm) que en R4 (12,6±10,3µm) (p<0,05). La mayor precisión lineal se observó en D2000 (7,2±7,6 µm) (p<0,05). La precisión angular de D2000 (0,02±0,015 grados) fue la más alta (p<0,01). La precisión angular de R4 (0,036±0,018 grados) fue la más baja (p<0,01). Este estudio reveló que la veracidad se vio afectada por la región del implante y la precisión se vio afectada tanto por LS como por la región del implante.

PALABRAS CLAVE: Digitalización; Precisión de escaneado; Escáneres de laboratorio; Cuerpo de escaneado de titanio; Pilar de varias unidades; Arcada completa.

INTRODUCTION

Implant-supported fixed dental prostheses (IFDPs) have been used to rehabilitate partially and completely edentulous patients, with high success rates (1). The passive fit of IFDPs is an essential factor to prevent biological and mechanical complications such as screw loosening and fracture, implant fracture, prosthetic component strain, and fracture or loss of the implant osseointegration (2). Although, a discrepancy threshold for the passive fit of IFDPs has not been consistent, the maximum discrepancy for an acceptable clinical fit was considered between 59 to 72μm (3). Better passive fit can be achieved by cement-retained IFDPs due to compensation of small misalignments and vertical gaps by cement (4), screw-retained IFDPs are widely used because of their advantages including reversibility, easier maintenance, and inadequate interocclusal space (5). Hybrid prostheses with multi-unit abutments (MUA) have become an effective prosthodontic option, which contributes to aesthetics and phonation with cheek and lip support, especially in the atrophic maxilla (6).

Computer-aided design and computer-aided manufacturing (CAD-CAM) technology present advantages for the passive fit of IFDPs compared with conventional fabricating techniques (7). To produce accurate high-quality IFDPs with CAD/CAM systems, laboratory scanners (LS) and intraoral scanners (IOS) are used for the acquisition of implant positions with the use of scan bodies as in CAD/CAM workflow (8,9). Scan bodies are made of polyetheretherketone, titanium alloy, aluminum alloy, and various resins with dull, smooth, and opaque surfaces to be easier to scan (10,11). Although it is considered that higher precision acquisition can be achieved with polyether ketone scan bodies, there was no significant difference between the accuracies of polyether ketone scan bodies and titanium scan bodies (12). Although, scan bodies fabricated by implant manufacturers

are usually used, third-party manufacturers also fabricate scan bodies by transferring the connection data between scan bodies and implants or analogs from implant manufacturers. Fabricating the scan bodies with connection data is essential for the accurate acquisition of implants (13). Therefore, in implant systems where third-party scan bodies are not available, scan bodies provided by the implant manufacturer are used. Most implant manufacturers produce and market only titanium scan bodies.

IOS have been successfully used for single implant-supported or short-span implant-supported restorations. However, the distance between the scan bodies, the depth of the implant, and the location within the scan can affect the accuracy of digital impressions (14). So, the conventional splinted pick-up technique has been suggested for complete arch implant-supported restorations (11,15-18). Despite the risk of dimensional changes of impression material and improper connection of the components (19-22), more accurate impressions can be performed with the splinted pick-up impression technique (8,9).

LS have higher precision than intraoral scanners (23). However, complete-arch (24,25) and single-tooth (26) gypsum model scans can be affected by the scanning technologies of LS. Implant scan accuracy studies are often performed to evaluate the effect of polyether ketone scan bodies instead of titanium scan bodies on accuracies of LS (12,27,28). The purpose of the study was to compare the trueness and precision of LS by comparing linear and angular distortions in the indirect acquisition of complete-arch implants with original titanium scan bodies. The first null hypothesis of this study was that linear trueness was not affected by LS and inter-implant distance and angulation, the second was that angular trueness was not affected by LS and inter-implant distance and angulation, the third was that linear precision of LS was not affected by inter-implant

distance and angulation, and the fourth was that angular precision of LS was not affected by inter-implant distance and angulation.

MATERIALS AND METHODS

PREPARATION OF THE MASTER MODEL

An edentulous maxillary plaster mold was poured with polymethylmethacrylate (Procryla, President Dental, München, Germany). Six implant analogs (Fixo, Oxy implant, Biomec, Lecco, Italy) were inserted at the sites #12, #22, #14, #24, #16, and #26. A laboratory surveyor was used to control the direction of each hole toward the longitudinal axis of the residual ridge and the depth of each implant analog. Implant holes were parallelly prepared in #14, #16, #24, and #26. Implant holes #12 and #22 were prepared at an angle of 10 degrees. The implant hole distance between #16 and #26 was 36mm and the others were approximately 12mm. Implant analogs were inserted and fixed in holes with polymethylmethacrylate. To produce a master model, an abutment-level impression coping (Impression coping transfer, Fixo, Oxy implant, Biomec, Italy) was connected to each implant analog and splinted by using self-curing acrylic resin (Pattern Resin™ LS, GC Corporation, Tokyo, Japan). Open-tray impression was performed using a custom tray with polyvinyl siloxane impression material (Hydrorise implant, Zhermack, Rovigo, Italy). After the impression material had completely polymerized, guide pins were loosened, and the impression tray was removed from the cast. An implant analog was connected to each impression coping. Artificial soft tissue (Gingifast Elastic, Zhermack, Italy) was formed around each analog and impression coping complex. The impression was poured into type IV dental stone (Elite Rock, Zhermack, Italy) and the master model was obtained (Figure 1).
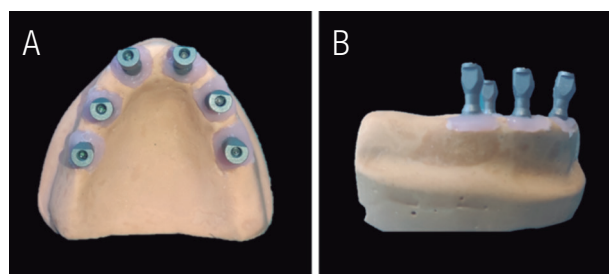

Figure 1. Images of the master model (A; occlusal view, B; lateral view).

COORDINATE-MEASURING MACHINE MEASUREMENT OF THE MASTER MODEL

The reference values of the master model were obtained using a coordinate-measuring machine (DEA Global Classic, Hexagon Metrology, Torino, Italy) (CMM) with an accuracy of 3μm. A high-accuracy sensing probe with a ruby stylus of 2mm diameter was used to measure the 3D position of the implant analogs by touching the cone-cylinder interface with a determined force. Geometric features and measured points were constructed using inspection software (PC-DMIS, Hexagon Metrology, Torino, Italy). To define the centroids of each multi-unit abutment (MUA) analog, 9 points were determined on the basis of the MUA analog and best-fitted into a sphere. The center of the sphere was defined as the centroid. A cone was defined for each analog by measuring 4 points for each of the two height levels on the MUA analogs. The angulation of each analog on the master model was determined toward the centre-axis of the cone. The linear distance (centroid to centroid) and angulation (centre-axis to centre-axis) between #16-14, #14-12, #12-22, #22-24, #24-#26, and #16-26 analogs were calculated. 3 repeated measurements were recorded for each analog and the mean of linear distance and angulation values were defined as reference values (27).

SCANNING PROCEDURE

Three laboratory scanners were compared in this study; D2000 (3Shape, Copenhagen, Denmark), Vinyl High Resolution (Smart Optics, Oslo, Norway), and inEos X5 (Dentsply Sirona, Konstanz, Germany). Six new grade-5 titanium scan bodies (Scan body, Fixo, Oxy implant, Biomec, Italy) were connected to the model and tightened with a calibrated torque ratchet (Torque ratchet, Fixo, Oxy implant, Biomec, Italy) at 15 Ncm. The master model was fixed on dental laboratory scanner. The number of scans per group to evaluate the scanning accuracy was identified using a power analysis software (G*Power 3.1.9.2, Duesseldorf, Germany) of data from a pilot experiment (n=5). It was found that 10 scans were necessary (power=95.52%, α=0.05). 10 scans for each laboratory scanner were performed repeatedly without detaching the model or the scan bodies. The acquired digital models were recorded in standard triangulation language (STL) format.

TRUENESS AND PRECISION ANALYSIS

Linear and angular trueness and precision were calculated by inspection software (Geomagic Control X, 2018, Geomagic, NC) according to ISO 17450-1-2-3 protocol;

1. STL models were digitally cropped so that only the polygon mesh of six scan bodies remained.
2. The top plane was defined by manually selecting meshes at the top of each scan body and associating a plane using a least-squares algorithm.
3. MUA plane was constituted by projecting the top plane in the negative Z-direction by the height of the scan body (12mm).
4. Centre-axis was defined by the centre-axis of the cylinder present in the scan body.
5. The centroid was defined as the intersection point of the centre-axis and MUA plane. Centre-axis and centroid were identified for each scan body (Figure 2).
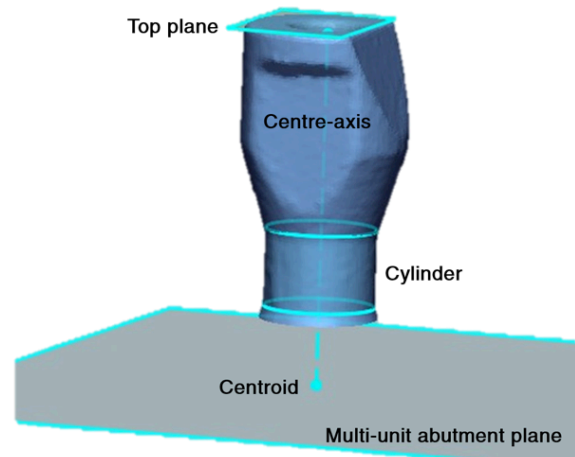

Figure 2. Virtual illustration of geometric features to define the centre-axis and centroid on the scan body.

Six linear distance (centroid to centroid) and six angulation (between centre-axes) measurements for each scan were performed between #16-14, #14-12, #12-22, #22-24, #24-26, and #16-26 scan bodies and were recorded (Figure 3). Implant regions were defined according to inter-implant distance and angulation; parallel (R1: #24-26 and #16-14), angled (R2: #22-24 and #14-12), angled to occlusal plane (R3: #12-22), and cross-arch (R4: #16-26). Trueness was defined as the closeness of linear distance and angulation measurements of LS to reference CMM. Precision was defined as the closeness of intra-group measurements of each LS.
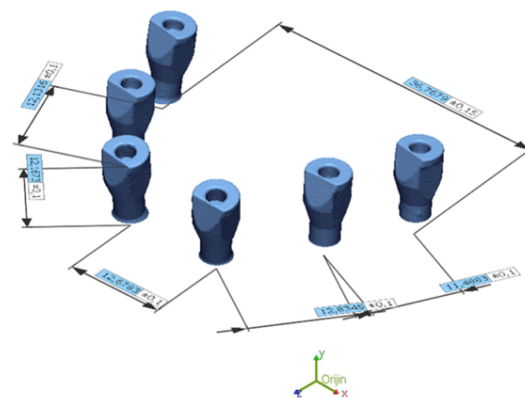

Figure 3. Example of a measured scan using Geomagic ControlX.

STATISTICS

All statistical values were analyzed using SPSS software (IBM SPSS Statistics for Windows, Version 22.0; IBM, Armonk, NY). A Shapiro-Wilk test was conducted to test intergroup normality, and the Levene test was conducted to test the homogeneity of variance (α=0.05). Two-way analyses of variance (ANOVA) were performed to evaluate the effect of LS and implant region on trueness. The post-hoc Scheffe test was used to compare the differences. The level of statistical significance was set at 0.05 for both statistical methods.

RESULTS

TRUENESS

Descriptive statistics of linear and angular distortions were presented in Table 1. A two-way ANOVA revealed that there was not a significant interaction between the effects of LS and region (F (6,168)=1.608, p=0.2021). LS did not have a significant effect on linear distortion (p=0.203). The mean linear distortion of D2000, Vinyl High Resolution, and inEOS X5 were 27.2±16μm,

31.6±24.1μm, and 30.6±24.9μm, respectively. The region had a significant effect on linear distortion (p<0.01). Significant lower linear distortion was noted on R3 (14.2±1.6μm) than on R2 (26±17.7μm) and R4 (61.2±17.9μm) (p<0.01). There were no significant differences between R3 and R1 (23.4±15.5μm) (p=0.428) and R1 and R2 (p=0.845). Significant greater linear distortion was noted in R4 compared to R1 (p<0.01) and R2 (p<0.01).

A two-way ANOVA revealed that there was a significant interaction between the effects of LS and region on angular distortion (F (6,168)=4.020, p<0.01). Simple main effects analysis showed that LS did not have a significant effect on angular distortion (p=0.403). Mean angular distortions of D2000, Vinyl High Resolution, and inEOS X5 were 0.051±0.021 degrees, 0.049±0.026 degrees, and 0.045±0.028 degrees, respectively. The region also did not have a significant effect on angular distortion (p=0.095). Mean angular distortions of R1, R2, R3, and R4 were 0.043±0.021 degrees, 0.049±0.025 degrees, 0.048±0.03 degrees, and 0.056±0.025 degrees, respectively. Scheffe post-hoc results were presented in Table 2.

Table 1. Descriptive statistics of linear distance distortions (mean (standard deviation) μm) and angulation distortions (mean (standard deviation) degrees).

		Parallel (R1)		Angled (R2)		Angled to occlusal plane (R3)	Cross-arch (R4)
		26-24	14-16	24-22	12-14	22-12	16-26
D2000	Linear distance	17.6(3,6)	31.1(10.1)	27.8(6.9)	26.3(8.7)	8.7(11)	51.8(12)
	Angulation	0.05(0.014)	0.032(0.02)	0.058(0.013)	0.035(0.021)	0.061(0.011)	0.07(0.016)
Vinyl High Resolution	Linear distance	14(11.5)	29.3(22.3)	30.2(16.4)	15.4(15.1)	21.1(13.8)	65.5(21.4)
	Angulation	0.044(0.016)	0.059(0.024)	0.051(0.019)	0.029(0.019)	0.042(0.038)	0.067(0.02)
In EOS X5	Linear distance	34(18)	14.1(7.5)	46.4(22.6)	10.2(6.6)	12.9(5.8)	66.2(16.9)
	Angulation	0.049(0.02)	0.025(0.012)	0.074(0.03)	0.05(0.023)	0.04(0.031)	0.032(0.021)

Table 2. Comparisons of linear distance distortions (mean (standard deviation) µm) and angular distortions (mean (standard deviation) degrees).

		R1	R2	R3	R4
D2000	Linear distance	24.4(10.1)[a]	27(7.7)[a]	8.7(11)[b]	51.8(12)[c]
	Angulation	0.041(0.019)[a]	0.046(0.021)[a]	0.061(0.011)[ab]	0.07(0.016)[b]
Vinyl High Resolution	Linear distance	21.7(19)[a]	22.8(17.1)[a]	21.1(13.8)[a]	65.5(21.4)[b]
	Angulation	0.051(0.021)	0.04(0.022)	0.042(0.038)	0.067(0.02)
In EOS X5	Linear distance	24.1(16.8)[a]	28.3(24.6)[a]	12.9(5.8)[a]	66.2(16.9)[b]
	Angulation	0.037(0.02)[ab]	0.062(0.029)[b]	0.04(0.031)[ab]	0.032(0.021)[a]

R1: #24-26 and #16-14, R2: #22-24 and #14-12, R3: #12-22, R4: #16-26. The different lowercase letters within the same row indicate statistical difference (Scheffe) (P<0.05).

PRECISION

A two-way ANOVA revealed that there was a significant interaction between the effects of LS and region (F (10,792)=6.705, p<0.01), LS (p<0.01), and region (p<0.01) on linear precision. The mean linear precision of D2000, Vinyl High Resolution, and inEOS X5 were 7.2±7.6µm, 12.7±9.7µm, and 11.1±8.8µm, respectively. The mean linear precision of D2000 was significantly lower than Vinyl High Resolution (p<0.01) and inEOS X5 (p<0.01). There was no significant difference between Vinyl High Resolution and inEOS X5 (p=0.087). Greater mean linear precision was noted in R1 (9±8µm) and R3 (9.3±8.3µm) than in R4 (12.6±10.3µm) (p<0.01 and p=0.02, respectively) There was no significant difference between R2 (10.9±9.4µm)-R4 (p=0.367), R1-R2 (p=0.078), and R2-R3 (p=0.318).

A two-way ANOVA revealed that there was a significant interaction between the effects of LS and region (F (10, 792)=48.102, p<0.01), LS (p<0.01), and region (p<0.01) on angular precision. The mean precision of D2000, Vinyl High Resolution, and inEOS X5 were 0.02±0.015 degrees, 0.032±0.019 degrees, and 0.033±0.018 degrees, respectively. The angular precision of D2000 was better than Vinyl High Resolution (p<0.01) and inEOS X5 (p<0.01). No difference was found between Vinyl High Resolution and inEOS X5 (p=0.827). Greater angular precision was noted in R3 (0.023±0.016 degrees) than in R1 (0.028±0.019 degrees) (p=0.046), and R4 (0.036±0.018 degrees) (p<0.01). There was no significant difference between R1 and R2 (0.028±0.018 degrees) (p=0.065). Greater angular deviations were noted in R4 than in R1 (p=0.004) and R2 (p=0.002). Scheffe post-hoc test results were presented in Table 3.

Table 3. Comparisons of linear precisions (mean (standard deviation) µm) and angular precisions (mean (standard deviation) degrees).

		R1	R2	R3	R4
D2000	Linear distance	4.6(3.7)[a]	5.8(3.9)[a]	10.7(11.4)[b]	11.5(10.6)[b]
	Angulation	0.019(0.013)[a]	0.017(0.012)[a]	0.016(0.011)[a]	0.033(0.018)[b]
Vinyl High Resolution	Linear distance	12.3(8.4)	13.2(10.8)	10.4(6.8)	14.8(11.8)
	Angulation	0.035(0.019)[a]	0.033(0.02)[a]	0.019(0.012)[b]	0.038(0.017)[a]
In EOS X5	Linear distance	10.2(8.9)[a]	13.9(9.6)[a]	9.3(8.3)[b]	12.6(10.3)[a]
	Angulation	0.031(0.019)	0.034(0.017)	0.034(0.018)	0.035(0.02)

R1: #24-26 and #16-14, R2: #22-24 and #14-12, R3: #12-22, R4: #16-26. The different lowercase letters within the same row indicate no statistical difference (Scheffe) (P<0.05).

DISCUSSION

According to the results of the present study, the linear trueness was not affected by both the interaction of LS and region (p=0.2021) and LS (p=0.203). On the other hand, the region affected linear trueness (p<0.01). While the interaction of simple effects (LS and region) affected the angular trueness (p<0.01), simple effects did not affect angular trueness (p=0.403, and p=0.095, respectively.). So, the first and the second null hypotheses were partially rejected. For precision, the main effects (region and LS) and their interactions affected both linear and angular distortions (p<0.05). So, the third and the fourth null hypotheses were rejected.

Different mean linear distortions were presented in studies with the use of different LS. Fluegge et al. (12) reported linear distortions between 6.2 to 14.1µm for short-span implant-supported restorations (D250; 3Shape, Denmark). Huang et al. (11) reported linear distortions between 35.35 and 52.58µm for four implants on mandible with original polyether ketone scan bodies (D2000; 3Shape, Denmark). Pan et al. (29) determined linear distortions on abraded aluminum experimental calibration block which imitated the all-on-4 concept (Zfx Evolution plus+, Zimmer Biomet, USA). Pan et al. (27) reported the linear distortions between 10.4 to 52µm with six polyether ketone third-party scan bodies on complete-arch (Zfx Evolution plus+, Zimmer Biomet, USA). Tan et al. (30) reported linear distortions between 11.1 to 45.4µm (inEOS X5). As can be seen from the studies mentioned above, single implants can be digitized with higher accuracy. Our linear distortion results were close to previous studies using polyether ketone scan bodies (11,27,30).

Although the linear distortions between the scan bodies with approximately 12mm inter-analog distance (8.7-28.3µm) have not reached the threshold of clinical significance (up to 72µm) (3), linear distortions in the cross-arch region (36mm inter-analog distance) (51.8-65.5µm) were closed to the threshold in the present study. Inter-implant distance generally affects the scan accuracy of IOS. Clinicians take multiple images to obtain a complete arch scan due to the limited viewpoint of IOS and the software stitches the images. Accumulate errors could come up because of the lack of reference points on the mucosa between implants (11). On the other hand, images are merged by coordinates in LS and the digital complete arch model can be established without stitching images (29). So, the effect of inter-implant distance on the accuracy of LS is not expected. However, Cho et al. (31) determined that the accuracy of LS decreases when the scanned area increases. Progressive errors and loosening accuracy can be induced unless multiple images merge by coordinates (32). Pan et al. (27) found the largest linear distortion (41.4µm) between anterior and posterior implants in the All-on-4 concept and explained this result by the interaction between angulation of implants and inter-implant distance. But in the present study, 2 posterior cross-arch implants were parallelly positioned. The results of the present study showed that the linear accuracy of LS was affected by the inter-implant distance which was consistent with previous studies (12,27).

A finite element analysis demonstrated that angular distortion may lead to more localized stress on bone due to the overloading of a superstructure and may cause bone resorptions (33). In the present study, neither LS (between 0.045 to 0.051 degrees) nor region (between 0.043 to 0.056 degrees) affected angular distortions. However, LS and region interaction affected angular distortion (p<0.01). Fluegge et al. (12) reported angular distortion between 0.03 to 0.16 degrees for short-span implant-supported restorations. Pan et al. (27) reported 0.06 degrees for complete-arch implant-supported restorations Tan et al. (30) reported between -1.620 to 0.054 degrees for complete-arch implant-supported restorations. Olea-vielba et al. (34) reported 0.02 to 0.09 degrees for complete-

arch implant-supported restorations. The tightening torque of the scan body ,which limits the variety of connection fit between scan bodies and analogs, is specified as the reason for angular distortions (12,27). However tightening torque of the scan body was unstandardized or unmentioned in most accuracy studies (9,14,34-37). In the present study, the tightening torque was applied by a standardized-torque wrench according to the manufacturer's recommendation, and scans were performed without loosening torque. The different results might be explained by the distortion of the material of the scan bodies (PEEK) due to higher tightening torque values (30) or scanning technologies of LS (24). Emir and Ayyildiz (24) determined that the accuracy of blue light scanners was higher than white light scanners and laser scanners. Blue light scanners that have higher precision due to shorter wavelengths were used in the present study.

Accuracy of acquisition is generally evaluated by two parameters such as trueness and precision. Trueness is defined as the deviation of the scanned object from its actual dimensions, while precision is the deviation between repeated scans. The present study was designed based on the principle of metrology. Analogs have available geometry to calculate the closest actual coordinates of the centre-axis and centroid by high accuracy CMM (14,27). By using this method, the actual divergences can be displayed which cannot be by using "best-fit algorithms" (38).

Limitations of this study were that one implant system, one type of scan body (grade 5 titanium), and a limited number of LS were investigated in the present study. The results of the study could not extrapolate to the other implant systems, LS, and scan bodies. Fixo (Oxy implants) supplies just titanium scan bodies. In the presented study, third-party polyether ketone scan bodies were not used. Fixo (Oxy implants) was recently released and connection data between the scan body and implant or analog might not be transferred to third-party manufacturers. Future studies are needed to evaluate the effect of original titanium scan bodies with different geometrical shapes of different implant systems on the accuracy of full-arch scanning.

CONCLUSION

With the limitations of the present study, it was concluded that the linear accuracy of laboratory scanners (D2000, Vinyl High Resolution, and inEOS X5) did not differ in complete-arch implants scans. Linear accuracy of laboratory scanners decreased with the increase in inter-implant distance. The linear distortions in the cross-arch region were close to the clinical tolerance. The interaction between laboratory scanners and implant regions affected angular accuracy. In the cross-arch region, the highest angular accuracy was determined inEOS X5.

AUTHOR CONTRIBUTION STATEMENT

Conceptualization and design: B.E and O.C.S.
Literature review: B.E.
Methodology and validation: B.E.
Formal analysis: B.E.
Investigation and data collection: B.E.
Resources: B.E. and O.C.S.
Data analysis and interpretation: B.E.
Writing-original draft preparation: B.E.
Writing-review & editing: O.C.S.
Supervision: O.C.S.
Project administration: B.E. and O.C.S.
Funding acquisition: B.E. and O.C.S.

ACKNOWLEDGMENTS

REFERENCES

1. Simonis P., Dufour T., Tenenbaum H. Long-term implant survival and success: a 10-16-year follow-up of non-submerged dental implants. Clin Oral Implants Res. 2010; 21: 772-7.

2. Carlson B., Carleson G.E. Prosthodontic complications in osseointegrated dental implant treatment. Implant Dent. 1994; 3 (4): 264.

3. Papaspyridakos P., Benic G.I., Hogsett V.L., White G.S., Lal K., Gallucci G.O. Accuracy of implant casts generated with splinted and non-splinted impression techniques for edentulous patients: An optical scanning study. Clin Oral Implants Res. 2012; 23 (6): 676-81.

4. Hebel K.S., Gajjar R.C. Cement-retained versus screw-retained implant restorations: Achieving optimal occlusion and esthetics in implant dentistry. J Prosthet Dent. 1997; 77 (1): 28-35.

5. Da Rocha P.V.B., Freitas M.A., De Morais Alves Da Cunha T. Influence of screw access on the retention of cement-retained implant prostheses. J Prosthet Dent. 2013; 109 (4): 264-8.

6. Kwon T., Bain P.A., Levin L. Systematic review of short- (5-10 years) and long-term (10 years or more) survival and success of full-arch fixed dental hybrid prostheses and supporting implants. J Dent. 2014; 42 (10): 1228-41.

7. Kapos T., Evans C. CAD/CAM Technology for Implant Abutments, Crowns, and Superstructures. Int J Oral Maxillofac Implant. 2014; 29: 117-36.

8. Kim K.R., Seo K. young, Kim S. Conventional open-tray impression versus intraoral digital scan for implant-level complete-arch impression. J Prosthet Dent. 2019; 122 (6): 543-9.

9. Knechtle N., Wiedemeier D., Mehl A., Ender A. Accuracy of digital complete-arch, multi-implant scans made in the edentulous jaw with gingival movement simulation: An in vitro study. J Prosthet Dent. 2022; 128 (3): 468-478.

10. Mizumoto R.M., Yilmaz B. Intraoral scan bodies in implant dentistry : A systematic review. J Prosthet Dent. 2018; 120 (3): 343-52.

11. Huang R., Liu Y., Huang B., Chen Z., Li Z. Improved scanning accuracy with newly designed scan bodies : An in vitro study comparing digital versus conventional impression techniques for complete-arch implant rehabilitation. 2020; 31: 625-33.

12. Fluegge T., Att W., Metzger M., Nelson K. A Novel Method to Evaluate Precision of Optical Implant Impressions with Commercial Scan Bodies-An Experimental Approach. J Prosthodont. 2017; 26 (1): 34-41.

13. Fokas G., Ma L., Chronopoulos V., Mattheos N. Differences in micromorphology of the implant e abutment junction for original and third-party abutments on a representative dental implant. J Prosthet Dent. 2019; 121 (1): 143-50.

14. Giménez B., Özcan M., Martinez-Rus F., Pradies G. Accuracy of a Digital Impression System Based on Parallel Confocal Laser Technology for Implants with Consideration of Operator Experience and Implant Angulation and Depth. Int J Oral Maxillofac Implant. 2014; 29: 853-62.

15. Rutkunas V., Gečiauskaite A., Jegelevičius D., Vaitiekunas M. Accuracy of digital implant impressions with intraoral scanners. A systematic review. Eur J Oral Implant. 2017; 10: 101-20.

16. Wulfman C., Naveau A., Rignon-Bret C. Digital scanning for complete-arch implant-supported restorations: A systematic review. J Prosthet Dent. 2020; 124 (2): 161-7.

17. Assunção W.G., Britto R.C., Ricardo Barão V.A., Delben J.A., Dos Santos P.H. Evaluation of Impression Accuracy for Implant at

Various Angulations. Implant Dent. 2010; 19 (2): 167-74.

18. Abdel-azim T., Zandinejad A., Elathamna E., Lin W., Morton D. The Influence of Digital Fabrication Options on the Accuracy of Dental Implant-Based Single Units and Complete-Arch Frameworks. Int J Oral Maxillofac Implant. 2014; 29 (6): 1281-8.

19. Conrad H.J., Pesun I.J., DeLong R., Hodges J.S. Accuracy of two impression techniques with angulated implants. J Prosthet Dent. 2007; 97 (6): 349-56.

20. Menini M., Setti P., Pera F., Pera P., Pesce P. Accuracy of multi-unit implant impression : traditional techniques versus a digital procedure. Clin Oral Invest. 2018; 22 (3): 1253-62.

21. Fernandez M.A., Mendoza C.Y.P. De, Platt J.A., Levon J.A., Hovijitra S.T., Nimmo A. A Comparative Study of the Accuracy between Plastic and Metal Impression Transfer Copings for Implant Restorations. J Prosthod. 2013; 22: 367-76.

22. Braian M., Bruyn C.D.T.H. De, Fransson H., Christersson C., Wennerberg A. Tolerance Measurements on Internal- and External-Hexagon Implants. Int J Oral Maxillofac Implant. 2014; 29 (4): 846-52.

23. Ender A., Mehl A. Accuracy of complete-Arch dental impressions: A new method of measuring trueness and precision. J Prosthet Dent. 2013; 109 (2): 121-8.

24. Emir F., Ayyıldız S. Evaluation of the trueness and precision of eight extraoral laboratory scanners with a complete-arch model: a three-dimensional analysis. J Prosthodont Res. 2019; 63 (4): 434-9.

25. Renne W., Ludlow M., Fryml J., Schurch Z., Mennito A., Kessler R., et al. Evaluation of the accuracy of 7 digital scanners: An in vitro analysis based on 3-dimensional comparisons. J Prosthet Dent. 2017; 118 (1): 36-42.

26. González de Villaumbrosia P., Martínez-Rus F., García-Orejas A., Salido M.P., Pradíes G. In vitro comparison of the accuracy (trueness and precision) of six extraoral dental scanners with different scanning technologies. J Prosthet Dent. 2016; 116 (4): 543-550.e1.

27. Pan Y., Tam J.M.Y., Tsoi J.K.H., Lam W.Y.H., Pow E.H.N. Reproducibility of laboratory scanning of multiple implants in complete edentulous arch: Effect of scan bodies. J Dent. 2020; 96 (January): 103329.

28. Chia V.A., Rcsed M.R.D., Esguerra R.J., Teoh K.H., Juin F, Teo W, et al. In Vitro Three-Dimensional Accuracy of Digital Implant Impressions : The Effect of Implant Angulation. Int J Oral Maxillofac Implant. 2017; 32 (2): 313-21.

29. Pan Y., Tam J.M., Tsoi J.K., Lam W.Y., Huang R., Chen Z., et al. Evaluation of laboratory scanner accuracy by a novel calibration block for complete-arch implant rehabilitation. J Dent. 2020; 102: 103476.

30. Tan M.Y., Sophia M.D.S., Xin H., Keng M.D.S., Wong M., Tan Y.H., et al. Comparison of Three-Dimensional Accuracy of Digital and Conventional Implant Impressions : Effect of Interimplant Distance in an Edentulous Arch. Int J Oral Maxillofac Implant. 2019; 34 (2): 366-80.

31. Cho S., Schaefer O., Thompson G.A., Guentsch A. Comparison of accuracy and

reproducibility of casts made by digital and conventional methods. J Prosthet Dent. 2015; 113 (4): 310-5.

32. Ender A., Mehl A. Accuracy of complete-arch dental impressions : A new method of measuring trueness and precision. J Prosthet Dent. 2013; 109 (2): 121-8.

33. Winter W., Mohrle S., Holst S., Karl M. Bone loading caused by different types of misfits of implant-supported fixed dental prostheses: a three-dimensional finite element analysis based on experimental results. Int J Oral Maxillofac Implant. 2010; 25 (5): 947-52.

34. Olea-vielba M., Jare D., Methani M.M. Accuracy of the Implant Replica Positions on the Complete Edentulous Additive Manufactured Cast. J Prosthod. 2020; 29 (9): 780-6.

35. Thanasrisuebwong P., Kulchotirat T., Anunmana C. Effects of inter-implant distance on the accuracy of intraoral scanner : An in vitro study. J Adv Prosthodont. 2021; 21 (13): 107-16.

36. Lee S.J., Kim S.W., Lee J.J., Cheong C.W. Comparison of intraoral and extraoral digital scanners: Evaluation of surface topography and precision. Dent J. 2020; 8 (2): 52.

37. Ebeid K., Nouh I., Ashraf Y., Cesar P. F. Accuracy of different laboratory scanners for scanning of implant-supported full arch fixed prosthesis. J Esthet Restor Dent. 2022; 34 (5): 843-848.

38. Güth J.F., Runkel C., Beuer F., Stimmelmayr M., Edelhoff D., Keul C. Accuracy of five intraoral scanners compared to indirect digitalization. Clin Oral Investig. 2017; 21 (5): 1445-55.